JPET Fast Forward. Published on February 8, 2005 as DOI: 10.1124/jpet.104.082560
This article has not been copyedited and formatted. The final version may differ from this version.

JPET #82560

PHARMACOKINETIC-PHARMACODYNAMIC MODELLING OF THE ANTINOCICEPTIVE EFFECT OF BUPRENORPHINE AND FENTANYL IN RATS: ROLE OF RECEPTOR EQUILIBRATION KINETICS

Ashraf Yassen, Erik Olofsen, Albert Dahan and Meindert Danhof

Leiden/Amsterdam Center for Drug Research, Division of Pharmacology, Gorlaeus Laboratory, Leiden, The Netherlands (A.Y., M.D.)

Department of Anesthesiology, Leiden University Medical Center, Leiden, The Netherlands (E.O., A.D.)

running title: PK/PD of buprenorphine and fentanyl

Address for correspondence:

Prof. Dr. Meindert Danhof

Leiden/Amsterdam Center for Drug Research

Division of Pharmacology, Gorlaeus Laboratories

P.O. Box 9502, 2300 RA Leiden, The Netherlands

E-mail: M.Danhof@lacdr.leidenuniv.nl

TEL: +31 71 527 6211

FAX: +31 71 527 6292

total number of pages: 50

number of tables: 7

number of figures: 8

number of references: 40

number of words in the *Abstract*: 246

number of words in the *Introduction*: 707

number of words in the *Discussion*: 1489

Abbreviations: PK/PD, pharmacokinetic/pharmacodynamic; OFV, objective function value; HPLC, high-performance liquid chromatography; LC/MS/MS, Liquid Chromatography/Mass Spectrometry/Mass Spectrometry; MTBE, Methyl tertiary-butyl ether

Section assignment: Neuropharmacology

JPET Fast Forward. Published on February 8, 2005 as DOI: 10.1124/jpet.104.082560
This article has not been copyedited and formatted. The final version may differ from this version.

ABSTRACT

The objective of this investigation was to characterise the pharmacokinetic/ pharmacodynamic (PK/PD) correlation of buprenorphine and fentanyl for the antinociceptive effect in rats. Data on the time course of the antinociceptive effect following intravenous administration of buprenorphine or fentanyl was analysed in conjunction with plasma concentrations by non-linear mixed effects analysis. For fentanyl the pharmacokinetics was described on the basis of a two-compartment pharmacokinetic model. For buprenorphine, a three-compartment pharmacokinetic model best described the concentration time course. To explain time-dependencies in pharmacodynamics of buprenorphine and fentanyl a combined effect compartment/receptor binding model was applied. A log-logistic probability distribution model is proposed to account for censored tail flick latencies. The model converged yielding precise estimates of the parameters characterizing hysteresis. The results show that onset and offset of the antinociceptive effect of both buprenorphine and fentanyl is mainly determined by biophase distribution. The k_{eo} was 0.024 min^{-1} (95 % CI: 0.018-0.030 min^{-1}) and 0.123 min^{-1} (95 % CI: 0.095-0.151 min^{-1}) for buprenorphine and fentanyl respectively. On the other hand, part of the hysteresis in the buprenorphine pharmacodynamics could be explained by slow receptor association/dissociation kinetics. The k_{off} was 0.073 min^{-1} (95 % CI: 0.042-0.104 min^{-1}) and k_{on} was 0.023 ml/ng/min (95 % CI: 0.013-0.033 ml/ng/min). Fentanyl binds instantaneously to the OP3 receptor as no reasonable values for k_{on} and k_{off} were obtained with the dynamical receptor model. The findings of this study show that, in contrast to earlier reports in the literature, the rate-limiting step in the onset and offset of buprenorphine's antinociceptive effect is distribution to the brain.

INTRODUCTION

Buprenorphine is semi-synthetic opiate synthesized from the precursor thebaine. Several studies have revealed OP3 (μ-opioid) receptor agonistic binding capacity for buprenorphine. More specifically, a study conducted in the spinal dog classified buprenorphine as a partial agonist for the OP3 receptor (Martin *et al.*, 1976). The OP3 receptor is of specific interest, given its role in the mediation of analgesia (Zhang and Pasternak, 1981; Lutfy *et al.*, 2003). In principle, partial agonists only produce a sub-maximal response relative to full agonists which display full efficacy. However, the exact behavior of buprenorphine at the OP3 receptor in relation to its analgesic effect has not yet been unequivocally clarified. Data from animal studies suggest that buprenorphine-mediated analgesia might be governed by a bell-shaped dose-response curve (Cowan *et al.*, 1977a,b; Dum and Herz, 1981). At the lower dose range a dose-dependent increase in analgesia is observed, while at intermediate doses the response is diminished. At relatively high doses evidence for an inverse dose-response relationship has been obtained in animals. However, the observed pharmacological behavior at high doses can not be explained by partial agonist activity. Furthermore, the existence of a bell-shaped dose-response relationship in human, remains controversial, based on the results of studies in volunteers and patients. On the basis of studies in humans it has been claimed that ceiling effect, for side effects as respiratory depression, may occur either within the therapeutic analgesic dose range or at doses exceeding the clinically relevant range, reflecting partial agonism (Walsh *et al.*, 1994). In addition, several studies have demonstrated full analgesic efficacy for buprenorphine over a wide dose range (Mok *et al.*, 1981; Watson *et al.*, 1982; Christoph *et al.*, 2005). Besides its intrinsic activity at the OP3 receptor, buprenorphine has another interesting characteristic with respect to OP3 receptor binding (Boas and Villiger, 1985; Cowan *et al.*, 1977a). The kinetics of binding to and dissociation from the OP3 receptor is slow. The slow receptor kinetics at the OP3 receptor are reflected by a slow onset and a prolonged duration of effect. The slow receptor kinetics

combined with its low intrinsic activity make buprenorphine an attractive compound for the treatment of opiate addiction as an alternative for methadone (Jasinski *et al.*, 1978). However, the slow receptor equilibration kinetics also attributes to the difficulty of naloxone to compete with buprenorphine for the OP3 receptor. Consequently, reversal of buprenorphine's effect with naloxone appears to be difficult (Gal, 1989). In contrast, fentanyl binds to and dissociates from the OP3 receptor rapidly. Observed hysteresis in concentration-effect data of fentanyl is typically explained by factors related to the blood-brain equilibration (Scott *et al.*, 1991). Surprisingly, despite the fact that buprenorphine and fentanyl have similar physico-chemical properties (high lipophilicity) nobody has addressed the question whether the kinetics of buprenorphine effect is also delayed by biophase distribution. Despite the increasing progress in receptor pharmacology and clinical pharmacology of opiates little information is available on the *in vivo* kinetics of drug action and more specifically the PK/PD correlation of buprenorphine and fentanyl. In recent years, there has been an increasing interest in the application of receptor theory in PK/PD modelling with the aim to predict *in vivo* concentration-effect relationships (Van der Graaf and Danhof, 1997). An important feature of these mechanism-based models is the strict distinction between drug -and system related properties (Van der Graaf *et al.*, 1999; Visser *et al.*, 2002; Zuideveld *et al.*, 2004). A common feature of these models is that rapid equilibration of the drug-receptor complex is assumed. However, some drugs do not bind rapidly with their pharmacological target and therefore the time course of drug effect is influenced by the kinetics of the target equilibration (Shimada *et al.*, 1996). In this investigation a mechanism-based PK/PD model is proposed which contains specific expressions for the kinetics of the drug-receptor interaction *in vivo*. A specific feature of the model is that it allows separation of the kinetics of biophase distribution from the receptor association/dissociation kinetics to explain time-dependencies in pharmacodynamics. Identification and quantification of the rate-limiting step for kinetics of drug action will improve the understanding of the differences in PK/PD

properties between buprenorphine and fentanyl, ultimately, also in relation to the kinetics of the interaction with naloxone. In the investigation, tail flick latency has been used as a response measure. The developed PK/PD model was evaluated and validated over a wide dosing range and by application of several infusion rates. Furthermore, the accuracy and precision of the pharmacokinetic model predictions was assessed by bootstrap analysis and a posterior predictive check.

METHODS

Animals

Male Wistar rats were used in all experiments. The animals were housed in plastic cages in groups before surgery and individually after surgery. The animals were housed under laboratory standard conditions at constant room temperature (21 °C) and on a 12-h light/dark cycle, with lights turned on at 0700 am and off at 0700 pm. Food (RMH-TM; Hope Farms, Woerden, The Netherlands) and acidified water were allowed ad libitum. The animals were handled and allowed for acclimation to the experimental environment for ten days prior to the start of the experiment. The protocol was approved by the Ethical Committee on Animal Experimentation of Leiden University.

Surgical Procedure

Surgery was carried out under anesthesia with an intramuscular injection of 0.1 mg/kg medetomidine hydrochloride (Domitor 1 mg/ml; Pfizer, Capelle a/d IJssel, The Netherlands) and 1 mg/kg Ketamine base (Ketalar 50 mg/ml; Parke-Davis, Hoofddorp, The Netherlands). Two days before the experiment indwelling cannulae were implanted, one in the left femoral artery and one in the right jugular vein. The cannula in the right jugular vein was used for administration of the opiate while the cannula in the left femoral artery was used for serial collection of arterial blood samples. The cannulae were made from pyrogen free, non-sterile polyethylene tubing. One day before surgery cannulae were disinfected in a benzalkoniumchlorid 1 % solution. The venous cannula consisted of 3 cm polyethylene tubing (0.28 mm i.d.; Portex Limited, Kent, United Kingdom) heat-sealed to 9 cm polyethylene tubing (0.58 mm i.d.; Portex Limited, Kent, United Kingdom). The arterial cannula consisted of 3 cm polyethylene tubing

(0.28 mm i.d.) heat-sealed to 21 cm polyethylene tubing (0.58 mm i.d.). The cannulae were tunnelled subcutaneously and fixed at the back of the neck with a rubber ring. The skin in the neck and throat was stitched with normal suture. The skin in the groin was closed with wound clips. In order to prevent clotting and cannula obstruction the cannulae were filled with a 25% (w/v) polyvinylpyrrolidone solution (PVP; Brocacef, Maarssen, The Netherlands) in pyrogen-free physiological saline (B. Braun Melsungen AG, Melsungen, Germany) containing 20 IU/ml heparin (Hospital Pharmacy, Leiden University Medical Center, Leiden, The Netherlands).

Drugs and dosages

Buprenorphine hydrochloride and fentanyl monocitrate were kindly donated by Grünenthal GmbH (Aachen, Germany). Buprenorphine hydrochloride solution was prepared in saline with aid of two drops polysorbate 80 (Hospital Pharmacy, Leiden University Medical Center, Leiden, The Netherlands). To accelerate solubility, the solution was placed in an ultra-sonification bath for 30 min. Fentanyl monocitrate solution was prepared in saline. The doses and concentrations of buprenorphine and fentanyl are expressed as free base.

Measurement of antinociceptive effect

A tail flick analgesia meter (Columbus Instruments, Columbus, Ohio, USA) was used to determine the pain sensitivity in the control and the drug-treated rats (D'Amour and Smith, 1941). Radiant heat was applied using a shutter-controlled lamp as a heat source focused on a spot located 6.5 to 7.5 cm from the tip of the tail. The intensity of the beam was set at a level producing basal latency times between 2.5 and 3.5 s. To prevent tissue injury, the cut-off time was fixed at 10 s. A digital response time indicator with a resolution of 0.1 s measured the time between activation of the light beam and the tail flick.

JPET Fast Forward. Published on February 8, 2005 as DOI: 10.1124/jpet.104.082560
This article has not been copyedited and formatted. The final version may differ from this version.

Drug analysis

Buprenorphine and norbuprenorphine plasma concentrations were determined by HPLC coupled to tandem mass spectrometry (LC/MS/MS). The chromatographic system consisted of an Agilent HP 1100 HPLC system (Agilent, Waldbronn, Germany) coupled to an API 4000 LC/MS/MS system (Applied Biosystems, Darmstadt, Germany). Chromatography was performed on a precolumn (Metaguard Polaris 3μ C18A 2 mm, Varian Darmstadt, Germany) guarded Synergi 4μ Hydro-RP 80A column 75 mm x 2 mm (Phenomenex, Aschaffenburg, Germany) at 40 °C and a flow rate of 0.8 ml/min. The mobile phase consisted of water (solvent A) and acetonitrile:tetrahydrofuran (90:10, v/v) (solvent B) both containing 0.1% formic acid. The programme started with 90% A for 1 min followed by a linear gradient from 90% A to 25% A ramped up in 4 min. After two minutes with 25 % A the gradient was switched back to 90 % A in 0.1 min. The system was equilibrated for 3 minutes before injecting the next sample. The total run time was set at 10.1 min. A retention time of 3.3 min for norbuprenorphine and 3.8 min for buprenorphine was found for both analytes and their respective deuterated internal standards. A plasma volume of 50 μl was used for the assay of rat samples, standards and quality control samples. All plasma samples (rat samples, standards and quality control samples) were spiked with 1 ng (25 μl of 4 μg/100 ml) of the internal standard ($^2H_4$-buprenorphine and $^2H_9$-norbuprenorphine). After adding 25 μl concentrated ammonia, the samples were extracted for 15 min by liquid/liquid extraction with 600 μl tert.-butyl methyl ether (MTBE). After centrifugation at 13200 rpm for 8 minutes, the organic phase was transferred to autosampler vials, evaporated to dryness at 40 °C under a gentle stream of nitrogen and reconstituted in 125 μl of 0.1% formic acid in acetonitrile:tetrahydrofuran (90:10, v/v). A volume of 50 μl was injected onto the HPLC column. For the construction of the calibration curve for buprenorphine and norbuprenorphine the following standard solutions were used: 0.047, 0.092, 0.19, 0.37, 0.73, 1.5, 2.9, 5.9 and 12 ng/ml. The calibration curve was linear in the range from 0.047 to 12 ng/ml

for both analytes (r>0.999). The lower limit of quantification (LLOQ) was 0.047 ng/mL for buprenorphine and norbuprenorphine. The accuracy ranged from 99.4 to 102.1 % for buprenorphine and from 96.1 to 101.0 % for norbuprenorphine. The precision for the determination of buprenorphine, expressed as coefficient of variation, ranged from 2.2 to 6.4 % for concentrations between 0.14 and 8.9 ng/mL. The respective values for norbuprenorphine are 2.0 to 3.7 % in the concentration range of 0.14 to 8.7 ng/mL.

Fentanyl plasma concentrations were analyzed using HPLC coupled to tandem mass spectrometry (LC/MS/MS). The chromatographic system consisted of an Agilent HP 1100 HPLC system (Agilent, Waldbronn, Germany) coupled to an API 3000 LC/MS/MS system (Applied Biosystems, Darmstadt, Germany). Chromatography was performed on a precolumn (Metaguard Polaris 3ţ C18A 2 mm, Varian Darmstadt, Germany) guarded Atlantis C18 column 3μ 100 mm x 2.1 mm (Waters, Eschborn, Germany). The mobile phase consisted of water (solvent A) and methanol (solvent B) both containing 0.5 % acetic acid. The programme started with 98% A for 2 min followed by a linear gradient from 98% A to 10% A ramped up in 1 min. After three minutes with 10 % A the gradient was switched back to 98 % A in 0.1 min. The system was equilibrated for 2.5 minutes before injecting the next sample. The total run time was set at 9.6 min. A retention time of 6.1 min for fentanyl and its deuterated internal standard. A plasma volume of 50 μl was used for the assay of rat samples, standards and quality control samples. All plasma samples (rat samples, standards and quality control samples) were spiked with 0.370 ng(25 μl of 14.8 ng/ml) of the internal standard ($^2H_5$-fentanyl). After adding 10 μl concentrated ammonia the samples were extracted for 15 min by liquid/liquid extraction with 600 μl tert.-butyl methyl ether (MTBE). After centrifugation at 13200 rpm for 8 minutes, the organic phase was transferred to autosampler vials, evaporated to dryness at 40 °C under a gentle stream of nitrogen and reconstituted in 125 μl of 0.5% acetic acid/methanol (90:10,v/v). A volume of 25 μl was injected onto the HPLC column. For the construction of the calibration curve for

fentanyl the following standard solutions were used: 0.118, 0.24, 0.47, 0.94, 1.9, 3.8, 7.5, 15, 30, 60 and 120 ng/ml. The calibration curve was linear in the range from 0.118 to 120 ng/ml ($r>0.999$). The lower limit of quantification (LLOQ) was 0.118 ng/mL. The accuracy ranged from 87.0 to 96.1 % and the precision from 1.9 to 4.0 % for concentrations in the range from 0.4 to 50.2 ng/mL.

Pharmacokinetic-pharmacodynamic experiments

To minimize the influence of circadian rhythms, all experiments started between 0900 and 0930 am. Animals were randomly assigned to the treatment groups. Detailed information regarding experimental design is presented in Table 1. Before administration of drug or vehicle four consecutive baseline tail flick latencies were obtained in each animal. The measurements were taken at a 15 min interval. The average of the four baseline latencies was taken as the basal latency time. Upon administration of buprenorphine or vehicle via a zero order intravenous infusion using an infusion pump (BAS Bioanalytical Systems Inc., West Lafayette, Indiana, USA), tail flick latency was measured at the following pre-defined time-points; dose I: 0, 5, 9, 14, 19, 24, 30, 40, 50, 95, 105, 125, 155 and 185 min after drug administration, dose II: 0, 5, 10, 14, 19, 24, 30, 40, 50, 65, 70, 95, 105, 125, and thereafter every 30 min till 305 min after drug administration, dose III: 0, 5, 10, 14, 19, 24, 30, 40, 50, 95, 105, 125 and thereafter every 30 min till 215 min after drug administration, dose IV: 0, 5, 10, 14, 19, 24, 30, 40, 50, 70, 90 and thereafter every 30 min till 420 min, dose V: 0, 5, 10, 14, 19, 24, 30, 40, 50, 70, 90, 150 and thereafter every 30 min till 510 min after drug administration. For fentanyl, antinociceptive measurements were performed at; dose I: 0, 3, 7, 13, 17, 23, 33, 45, 75, 105, 150, and 180 min, dose II: 0, 3, 7, 13, 17, 23, 33, 45, 55, 75, 105 and 135 min, dose III: 0, 3, 7, 13, 17, 23, 33, 45, 55, 75, 105, 135, 150, 180 and 210 min, dose IV: 0, 5, 15, 25, 35, 43, 55, 65, 80, 105, 150 and 180 min, dose V: 0, 3, 7, 17, 23, 33, 45, 55, 75, 95, 135, 150, 210 and 240 min

after drug administration. In cases where blood sampling coincided with the tail flick latency measurement, tail flick latency measurement preceded blood sampling to minimize stress for the animals. Before start of the infusion a blank blood sample (100 μl) was withdrawn. Each blood sample withdrawn was replaced by an equal volume of heparinized 0.9 % saline (20 IU heparin/ml). This procedure has minimal effects on the pharmacokinetics. In a separate study it has been demonstrated that the values of the pharmacokinetic parameters obtained in this manner were identical to those obtained in a separate (pilot) study without replacement of the collected blood (unpublished observations). Serial arterial blood samples were collected in heparinized microtubes. Plasma (50 μl) was separated from the blood by centrifugation at 5000 rpm for 15 min and frozen at -20 °C until analysis.

PK-PD modelling procedure

The pharmacokinetic and pharmacodynamic parameters of buprenorphine and fentanyl were estimated using non-linear mixed-effects modelling as implemented in the NONMEM software version V, level 1.1 (Beal and Sheiner, 1999). The population analysis approach, which takes into consideration both intra-animal and inter-animal variability, was undertaken using the first-order conditional estimation method with η-ε interaction (FOCE interaction) for pharmacokinetic analysis. All fitting procedures were performed on an IBM-compatible computer (Pentium IV, 1500 MHz) running under Windows NT with the Fortran compiler Compaq Visual Fortan version 6.1. An in-house available S-PLUS 6.0 (Insightful Corp., Seattle, WA, USA) interface to NONMEM version V was used for data processing and management (including automated posterior predictive check and bootstrap) and graphical data display.

Pharmacokinetic analysis

In order to determine the basic structural pharmacokinetic model for buprenorphine and fentanyl one-, two -and three compartment models were tested. Model selection and identification was based on the likelihood ratio test, pharmacokinetic parameter point estimates and their respective confidence intervals, parameter correlations and goodness-of-fit plots. For the likelihood ratio test, the significance level was set at α=0.01, which corresponds with a decrease of 6.6 points, after the inclusion of one parameter, in objective function value (OFV) under the assumption that the difference in OFV between two nested models is χ^2 distributed. The following goodness-of-fit plots were subjected to visual inspection to detect systemic deviations from the model fits: individual observed *vs.* population or individual predicted values and weighted residuals *vs.* time or population predicted values. On the basis of model selection criteria, two -and three compartment models were selected for fentanyl and buprenorphine, respectively. The pharmacokinetic analysis for the selected compounds was performed by use of the ADVAN3 TRANS4 and ADVAN11 TRANS4 subroutines in NONMEM. For example, for fentanyl, the pharmacokinetic parameters, clearance (*Cl*), the inter-compartmental clearance (*Q*) and the volumes of distribution of compartments 1 and 2 (V_1 and V_2) were estimated.

The stochastic part of the model was selected to describe inter-animal variability in pharmacokinetic parameters and assumed a log-normal distribution of all model parameters over the population. Therefore an exponential distribution model was used to account for inter-animal variability:

$$P_i = P_{tot} \cdot \exp(\eta_i) \quad (1)$$

in which P_i is the individual value of model parameter P, P_{tot} is the typical value (mean population value) of parameter P in the population, and η_i is the normally distributed inter-animal random variable with mean zero and variance ω^2. The coefficient of variation of the struc-

JPET Fast Forward. Published on February 8, 2005 as DOI: 10.1124/jpet.104.082560
This article has not been copyedited and formatted. The final version may differ from this version.

tural model parameters is expressed as percentage of the root mean square of the inter-animal variance term. Selection of an appropriate residual error model was based on inspection of the goodness-of-fit plots. On this basis a proportional error model was proposed to describe residual error in the plasma drug concentration:

$$C_{obs,ij} = C_{pred,ij} \cdot (1 + \varepsilon_{ij}) \tag{2}$$

in which $C_{obs,ij}$ is the jth observed concentration in the ith individual, $C_{pred,ij}$ is the predicted concentration, and ε_{ij} is the normally distributed residual random variable with mean zero and variance σ^2. The residual error term contains all the error terms which can not be explained and refers to for example measurement and experimental error (e.g. error in recording sampling times) and structural model mis-specification. Individual empirical Bayes estimates of the pharmacokinetic parameters were obtained from the basic pharmacokinetic model and served as input for the pharmacodynamic model.

To refine the stochastic model, correlation between pharmacokinetic parameter estimates was tested by conducting covariance matrix analysis (OMEGA BLOCK option). A significant correlation between two parameters was assumed when the drop in OFV was more than 6.6 points ($p < 0.01$). Finally, explorative graphical analysis was performed to explore relationships between body weight and pharmacokinetic parameters. The following equation was used to model the pharmacokinetic parameters as function of bodyweight (BW):

$$P_i = \theta_i + \theta_j \cdot (BW - \text{median } BW) \tag{3}$$

in which P_i is the individual value of model parameter P, θ_i and θ_j are the intercept and slope of model parameter P *vs.* bodyweight relationship, respectively. To demonstrate the precision and stability of the pharmacokinetic models and to ascertain accurate prediction of concentration-time profiles of fentanyl and buprenorphine, the final population pharmacokinetic models were

subjected to an internal validation (Ette *et al.*, 2003; Food and Drug Administration, 1999). The validation procedure consisted of two components: bootstrap validation procedure and a posterior predictive check. For the bootstrap validation procedure, one thousand data sets were generated randomly sampled from the original data set with replacement. Subsequently, the final population PK models were fitted to the bootstrap replicates one at a time. Finally, the mean, standard error, coefficient of variation and 95 % confidence intervals of all model parameters were calculated and compared to parameter values obtained from the original study. To assess the predictive performance of the population PK models, one thousand data sets were simulated from the original data set and the final model parameter estimates. The median outcome and the 2.5 % and 97.5 % quantiles were calculated from the simulated buprenorphine and fentanyl concentrations at the pre-defined time-points.

Mechanism-based PK/PD analysis

In this study, the tail flick latency is used as a measure of the drug response. The mechanism-based model describing the complex relationship between drug concentration and pharmacological effect is displayed in figure 1. The observed hysteresis in concentration-effect data is traditionally explained by incorporation of a link model. In this model distribution to the biophase is characterized as first-order process, which is believed to constitute a correct representation of the rate-limiting step in the *in vivo* pharmacodynamics. Separation of different biological processes, causing hysteresis (i.e. biophase equilibration, receptor/association and transduction), frequently results in the inability to obtain unique parameter estimates expressing the respective rate-limiting steps (Tuk *et al.*, 1997, 1998; Cleton *et al.*, 1999). To explain hysteresis on the basis of two biological processes, the availability of a detailed data set including different doses and infusion schemes is required. Furthermore, with the anti-nociceptive effect as a pharmacodynamic endpoint the data analysis is complicated by the presence of censored

JPET Fast Forward. Published on February 8, 2005 as DOI: 10.1124/jpet.104.082560
This article has not been copyedited and formatted. The final version may differ from this version.

data (tail flick latencies above the cut-off value). To allow for estimation of the effect above the censoring value a maximum likelihood parameter estimation approach was used. This approach requires the specification of a probability distribution for the time at which an animal responds to applied radiant heat. In the statistical literature, several distributions have been proposed to describe time-to-event (also called survival) data; factors such as flexibility and practical implementation (i.e. in NONMEM) suggest the log-logistic and Weibull distributions as suitable candidates (Cox and Oakes, 1984). The log-logistic distribution is characterized by the median time to response (prediction) and a shape factor determining its width (Z). The probability of observing a tail flick latency > 10 s is given by the area under the log-logistic curve from 10 s to infinity. So the log likelihood to be maximized is the sum of terms of either:

$$\begin{aligned} \log\ \mathrm{P}\{\text{latency} = \text{observation}\} &= \log(Z) + (Z-1)\cdot\log\left(\tfrac{\text{observation}}{\text{prediction}}\right) - \\ &\quad 2\cdot\log\left(1+\left(\tfrac{\text{observation}}{\text{prediction}}\right)^{Z}\right) \qquad (4) \end{aligned}$$

or

$$\log\ \mathrm{P}\{\text{latency} > \text{cut}-\text{off}\} = -\log\left(1+\left(\tfrac{\text{observation}}{\text{prediction}}\right)^{Z}\right) \qquad (5)$$

The exposure-response relationships of buprenorphine and fentanyl are quantified using a mechanism-based PK/PD model. This model describes the equilibration to the biophase, where the drug can bind to the OP3 receptor. Drug distribution to the site of action (biophase) was characterized on the basis of an effect compartment model (Sheiner *et al.*, 1979). The rate of change of biophase drug concentrations can be described as follows:

$$\frac{d[C_e]}{dt} = k_{\mathrm{eo}}\cdot([C_p]-[C_e]) \qquad (6)$$

where k_{eo} is a first-order distribution rate constant describing the rate of change of drug con-

centration in the effect compartment and [C_p] represents the plasma concentration and [C_e] the effect-site concentration. At the site of action, the drug can bind to the OP3 receptor. Following the law of mass action, the rate of drug-receptor binding (d[C_eR]/dt) is proportional to the drug concentration [C_e] and the free receptor concentration [R]:

$$\frac{d[C_eR]}{dt} = k_{on} \cdot [C_e] \cdot [R] - k_{off} \cdot [C_eR] \tag{7}$$

in which k_{on} is a second-order rate constant describing the rate of association and k_{off} is a first-order rate constant describing the rate of dissociation of the drug-receptor complex. Under the assumption that the concentration of drug is in excess compared to the free receptor concentration and that the total number of receptors ([R_{tot}]) is equal to the sum of drug-bound receptors ([C_eR]) and unbound receptors ([R]), equation 7 can be rearranged into:

$$\frac{d[C_eR]}{dt} = k_{on} \cdot [C_e] \cdot ([R_{tot}] - [C_eR]) - k_{off} \cdot [C_eR] \tag{8}$$

The total amount of receptors ([R_{tot}]) could not be measured *in vivo* and therefore was set to one unity. Receptor binding was directly related to the tail flick latency time according to the following equation:

$$\text{prediction} = \frac{E_0}{1 - [C_eR]} \tag{9}$$

The concentration-effect data for fentanyl were analyzed by the following model (Sarton *et al.*, 2000):

$$\text{prediction} = E_0 \cdot \left[1 + \left(\frac{[C_e]}{[C_{100}]}\right)^{\gamma}\right] \tag{10}$$

where E_0 is the baseline tail flick latency, [C_{100}] the effect-site concentration causing 100 % increase in tail flick latency, and γ a slope parameter. This equation follows from the steady-state solution of equations 8 and 9 in which case k_{on} and k_{off} are not both identifiable (C_{100} = k_{off}/k_{on})

RESULTS

Buprenorphine and fentanyl pharmacokinetics

A two compartment model best described the pharmacokinetics of fentanyl, while for buprenorphine a three-compartment model was selected. The observed and population predicted concentration -time courses of buprenorphine and fentanyl are depicted in figure 2 and 3, respectively. All pharmacokinetic parameters were estimated precisely with acceptable coefficient of variance. For buprenorphine the coefficient of variation of the various parameters varied between 2.4 % and 32 %, while for fentanyl the range was between 2.5 % to 19 %. Estimation of inter-animal variability was possible for the following parameters: Cl, V_1,V_2 and V_3 of buprenorphine. For fentanyl inter-animal variability was estimated for Cl, V_1 and V_2. An overview of the values of the pharmacokinetic parameters and their respective coefficients of variation and inter-animal variability is provided in table 2 and table 3. Covariate analysis revealed a linear relationship between Cl, V_1, V_2 and V_3 *vs.* bodyweight (BW) and Cl *vs.* bodyweight for buprenorphine and fentanyl, respectively. The equations describing the covariate- pharmacokinetic parameter relationships are shown in table 4. The correlations between the values of inter-animal variability of Cl, V_1, V_2 and V_3 of buprenorphine and Cl, V_1, and V_2 of fentanyl were evaluated by using a full omega matrix. Subsequently, the full omega matrix was reduced to a matrix only including significant correlations between parameters. An increase of > 6.6 points of OFV was used to evaluate the significance of any correlation between the parameters after deletion of the respective covariance term. A correlation was observed between $\omega^2 Cl$ and $\omega^2 V_2$ of fentanyl and therefore the covariance of those parameters was added to the final model. The correlation coefficient between the two parameters was 0.70.

Finally, to validate the pharmacokinetic models a bootstrap validation and a posterior predictive check were conducted. The final population pharmacokinetic estimates for buprenor-

phine and fentanyl were nearly identical to the estimates obtained by fitting one thousand data sets to the final population PK models. Also, the estimated inter-animal variability for the final pharmacokinetic parameters was supported by the bootstrap validation (tables 2 and 3). The results of the posterior predictive check showed that the population PK models could well predict the time course of buprenorphine and fentanyl concentration after intravenous administration (figure 4).

Mechanism-based PK/PD model

After start of infusion, the maximal effect for fentanyl was reached after 25 min, while for buprenorphine maximal effect was reached after 50 min. The maximal peak effects obtained were different between buprenorphine and fentanyl, in spite of similarities in the concentration range studied. In the buprenorphine group IV the predicted peak effect was higher than predicted in group V, in spite of a lower dose. For buprenorphine the values of the maximal predicted tail flick latency ($\pm$ SEM) were 4.65 $\pm$ 0.11, 10.03 $\pm$ 0.54, 5.82 $\pm$ 0.90, 16.36 $\pm$ 1.92 and 14.71 $\pm$ 1.97 s for dose I-V, respectively. For fentanyl, a dose-related increase in the predicted peak effect was observed. The values of the maximal predicted tail flick latency were 7.26 $\pm$ 0.17, 13.17 $\pm$ 2.24, 15.11 $\pm$ 1.7, 7.95 $\pm$ 1.05, 21.49 $\pm$ 3.07 s for dose I-V, respectively. NONMEM analysis revealed that the correlation between the estimates of *in vivo* potency and E_{max} was highly correlated and consequently the PK/PD models were very unstable. Therefore, the intrinsic activity of buprenorphine and fentanyl could not be estimated. Simplification of the model assuming a linear concentration -or receptor binding-response relationship adequately described the data and led to a more stable model. The predicted tail flick latencies above the cut-off value of 10 s were estimated on the basis of a time-to-event analysis. The log-logistic and the Weibull probability distribution models were explored to account for censored time to response values. With the Weibull distribution incorporated, the model converged

successfully, yielding pharmacodynamic parameters estimates comparable with those obtained with the log-logistic distribution model. However, the latter model was superior to the Weibull model as judged by considerable run-time reduction and fitting performance. For instance, the objective function was -435 *vs.* 2000 for the log-logistic and the Weibull model, respectively. The time course of antinociceptive effect for both buprenorphine and fentanyl were analyzed using the developed 'biophase distribution/receptor binding' model and an effect compartment model. The buprenorphine *in vivo* data in this study supported the mechanism-based PK/PD model as indicated by the obtained objective function value (table 7). The population estimates were assessed as well as inter-animal variability. All the model parameters, structural and stochastic, were estimated precisely as indicated in table 5. On the other hand, the fentanyl effect *vs.* time data were equally well described with the effect compartment model and the combined 'biophase equilibration/receptor binding' model. Noteworthy, when applying the combined PK/PD model to the fentanyl plasma concentration-tail flick latency data, NONMEM continued iterating while no significant change in objective function was observed after 50 iterations. During further iteration process, parameter estimates of k_{on} and k_{off} were rising to high values. This implies that fentanyl binding to and dissociation from the OP3 receptor occurs rapidly and that the concentration-effect relationship can be characterized under equilibrium conditions. On the other hand, the estimate of k_{eo} was stable and did not change during further iteration. Therefore, information on the PK/PD correlation of fentanyl were obtained with the most parsimonious model, which is the effect compartment model. The pharmacodynamic parameters estimates of fentanyl are presented in table 6. The combined 'biophase equilibration/receptor binding' model and effect compartment model were able to successfully describe all individual effect *vs.* time profiles, yielding estimates of k_{eo}, k_{on} and k_{off} for buprenorphine and of k_{eo} for fentanyl. A summary of the goodness-of-fit of the effect compartment, receptor association/dissociation and combined biophase equilibration/receptor association dissociation

model with respect to the exposure-response relationships of buprenorphine and fentanyl is provided in table 7. Figure 5 and 6 show the time course of antinociceptive effect of buprenorphine and fentanyl, respectively and figure 7 shows the steady-state receptor binding -and effect-site concentration-antinociceptive effect relationship for both opiates. The population k_{on} and k_{off} were estimated at 0.023 ml/ng/min (95 % CI: 0.013-0.033 ml/ng/min) and 0.073 min^{-1} (95 % CI:0.042-0.104 min^{-1}). The biophase equilibration rate constant was 0.024 min^{-1}(95 % CI: 0.018-0.030 min^{-1}), which corresponds to $t_{1/2,keo}$ = 28.6 min. For fentanyl population k_{eo} was estimated at 0.123 min^{-1} (95 % CI: 0.095-0.151 min^{-1}), which corresponds to $t_{1/2,keo}$ = 5.6 min. A bootstrap analysis was not conducted for the validation of the population PK/PD models, due to long run times of the respective models in NONMEM. A posterior predictive check was not performed to assess the accuracy of the population PK/PD models, since this validation procedure does not provide additional information on the accuracy of the measured tail flick latency above the value of 10 s. Finally, no significant correlations between the pharmacodynamic parameter estimates or the inter-animal variability terms were observed.

DISCUSSION

A population PK/PD model for (semi-) synthetic opiates is proposed, which allows separate characterization of the kinetics of target site distribution and the receptor association/dissociation kinetics as determinants of the time course of the anti-nociceptive effect. It is shown that for buprenorphine both the target site distribution and the receptor binding kinetics contribute to the observed hysteresis between plasma concentration and effect while for fentanyl, hysteresis is determined by target site distribution only. The pharmacokinetics of buprenorphine and fentanyl were successfully described by a three -and two-compartment model, respectively. All pharmacokinetic parameters, including the estimated stochastic model parameters were estimated precisely, as indicated by the obtained standard errors. Both compounds share similar pharmacokinetic characteristics, with moderate to large steady-state volumes of distribution (0.6 to 1.5 l) and high hepatic clearance values (15 to 20 ml/min for rat weighting 300 g). The high clearance values found for buprenorphine and fentanyl approximate the rat hepatic blood flow and support blood-flow limited clearance of fentanyl and buprenorphine found in human (Stanski, 1987; Bullingham *et al.*, 1980). Finally, PK model validation demonstrated the accurateness and precision of the developed population PK models.

The PK/PD correlation of buprenorphine and fentanyl was determined in the rat using the effect of radiant heat on tail flick withdrawal as a pharmacodynamic endpoint. Characterization and prediction of the time course of drug effect was complicated by the presence of censored time to response values, which is an inherent limitation of the applied tail flick rat model. To integrate censored data (latencies above 10 s) in the PK/PD analysis, tail flick latencies were assumed to be log-logistically distributed and a maximum likelihood parameter estimation approach was used. A similar approach had been successfully applied in other studies (Luks *et al.*, 1998; Sarton *et al.*, 2000). An alternative for the log-logistic distribution is the Weibull distribution, which is also often used to describe time-to-event data. From the better performance

of the log-logistic distribution in comparison to the Weibull distribution it is concluded that the former better matches the actual distribution of the observed tail flick latencies.

The present study provides novel information on the pharmacokinetic/ pharmacodynamic relationship of buprenorphine and fentanyl. Considering the time course of drug action, usually a combination of different processes is involved in time delays of the biological effect intensity relative to plasma concentration. However, it is often difficult to extract and discriminate those processes from the available PK/PD data (Jusko *et al.*, 1995; Verotta and Sheiner, 1995; Cleton *et al.*, 1999). In this study, the separation of biophase kinetics from the *in vivo* receptor kinetics is an important feature of the mechanism-based PK/PD model. It is shown that with values of the half life of biophase equilibration ($t_{1/2,k_{eo}}$) and the receptor dissociation ($t_{1/2,k_{off}}$) of 29 min and 9 min respectively, the rate of onset and offset of antinociceptive effect is predominantly determined by distribution of buprenorphine to the effect site, as is also the case with fentanyl. However, in contrast to fentanyl, the contribution of the slow association/dissociation of buprenorphine to the OP3 receptor is not negligible. The half life of biophase equilibration ($t_{1/2,k_{eo}}$) for fentanyl was 5.6 min. These results are consistent with the idea that time-dependencies in fentanyl effect can be attributed to blood-brain concentration equilibration. The value of the half-life for biophase equilibration of fentanyl is remarkably similar to values reported by Scott *et al.* (1991) and Cox *et al.* (1998) who showed that the half life of blood-brain equilibration is 6.6 and 2.2 min, in rats and human respectively, using EEG effect as pharmacodynamic endpoint. Remarkably, the similarity of these values in human and rat suggests that the rate constant of biophase equilibration of fentanyl is, independent of species, similar for the EEG effect and for antinociception. Due to its high lipophilicity, it is believed that fentanyl penetrates the blood-brain barrier readily (Henthorn *et al.*, 1999). It is reasonable to assume that after blood-brain barrier passage, fentanyl distributes into the brain tissues before it is released to bind to the OP3 receptor. Since both compounds are highly

lipophilic, it is likely that buprenorphine distributes to the OP3 receptor in a similar manner, albeit that the values of the rate constants can be different.

The association/dissociation kinetics of buprenorphine at the OP3 receptor have also been determined *in vitro* (Boas and Villiger, 1985; Villiger and Taylor, 1982). Based on those receptor binding studies two binding affinity sites for buprenorphine have been identified. Dissociation of buprenorphine was characterized by an initial rapid phase ($t_{1/2,k_{off}}$ = 5.6 min.) followed by a slower phase ($t_{1/2,k_{off}}$ = 166.4 min.). The estimated *in vivo* dissociation half life for buprenorphine of 9.5 min is in the range of the reported value for the initial rapid phase of the dissociation from the buprenorphine-OP3 receptor complex *in vitro*. More important, the estimated *in vivo* equilibration constant K_D for buprenorphine, 3.20 ng/ml, corresponding to 6.85 nM, is in the same range as the *in vitro* dissociation equilibration constant, for which the values of 0.12 nM for the high affinity binding site and 1.38 nM for the low affinity binding site in the spinal cord and 1.0 nM for the binding site in the brain have been reported (Villiger and Taylor, 1982). It should be noted that the estimated *in vivo* K_D is calculated on basis of total plasma concentrations. Correction for the free fractions in plasma will result in an even greater similarity of the K_D values. For buprenorphine, no information on the free fraction is available which can be explained by the physicochemical properties of buprenorphine. Notably, the lipophilicity of buprenorphine complicates accurate measurement of the free fraction (sticking of buprenorphine to the membrane filter).

These results demonstrate the usefulness of this mechanism-based PK/PD model to explore *in vitro-in vivo* K_D correlations. Similar correlations have been reported for calcium channel antagonists using a receptor association/dissociation model (Shimada *et al.*, 1996) and also for A_1 adenosine receptor agonists and $GABA_A$ receptor modulators using a different mechanism-based PK/PD model based on receptor theory (Van der Graaf *et al.*, 1999; Visser *et al.*, 2003). Moreover, the ability to estimate an *in vivo* K_D allows a strict quantitative comparison with

the antinociceptive effect of other compounds. An important issue is the potency and intrinsic activity of buprenorphine relative to fentanyl. Interestingly, estimates of *in vivo* potency of buprenorphine and fentanyl are in close agreement and show that both compounds display equi-antinociceptive potency (3.20 *vs.* 3.51 ng/ml). The estimated C_{100} for fentanyl is obtained from equation 10. This equation follows from the steady-state solution of equations 8 and 9 in which case k_{on} and k_{off} are both not identifiable. Under steady-state conditions C_{100} equals $k_{off}/k_{on} = K_D$ and therefore K_D and C_{100} can be used to compare *in vivo* potency of buprenorphine and fentanyl. In addition, also the relative *in vivo* potency of drug and metabolite or drugs exhibiting enantiomeric isoforms can be explored using an integrated mechanism-based PK/PD modelling approach (Zuideveld *et al.*, 2002). For instance, it is postulated that buprenorphine's major metabolite, norbuprenorphine possesses a 50-fold weaker antinociceptive activity than the mother compound (Ohtani *et al.*, 1995). In the present study, the plasma concentrations of buprenorphine's major metabolite, norbuprenorphine, were also measured. However, the norbuprenorphine plasma concentrations were far below the concentration range, reflecting buprenorphine's antinociceptive effect (figure 8). Therefore, it was assumed that the contribution of norbuprenorphine to the overall analgesic effect is minimal.

An important question is whether buprenorphine acts as a full agonist (i.e. displays full antinociceptive effect). Mechanism-based PK/PD models provide an unique basis to characterize the effects of drugs in terms of *in vivo* potency and intrinsic activity (E_{max}). In recent years this approach has been successfully applied to explore the concentration-effect relationships of several compounds belonging to different drug classes (Van der Graaf *et al.*, 1999; Visser *et al.*, 2002). In the present investigation, maximal antinociceptive effect could not be estimated from the concentration-effect relationships. We relate this to the fact that, in this tail flick rat model stronger stimuli lead to a higher response, ultimately leading to complete antinociception. Consequently, no E_{max} is observed and no distinction can be made between partial and

full antinociceptive response during analysis. Furthermore, drug efficacy estimation is hampered by the fact that above the cut-off value only a probability distribution-based prediction of the antinociceptive behavior is provided. For some animals receiving the highest buprenorphine dose (0.1 mg/kg), the maximal predicted tail flick latency time is equal to or lower than the maximal predicted tail flick latency time resulted from 0.06 mg/kg administration. This seems consistent with data derived from previous animal studies supporting the concept of ceiling effect for antinociception (Cowan *et al.*, 1977a,b; Dum and Herz, 1981). However, on the basis of the present results no conclusions can be drawn regarding an eventual difference in the intrinsic efficacy of buprenorphine relative to fentanyl.

In conclusion, a mechanism-based PK/PD model has been successfully applied to the antinociceptive effect of buprenorphine and fentanyl. The model was able to separate biophase equilibration and receptor kinetics. In this respect it has been shown that the onset and offset of antinociceptive effect of buprenorphine and fentanyl are mainly determined by biophase equilibration. This mechanism-based PK/PD model can be extended in the characterization of buprenorphine's kinetics of action with respect to its respiratory inhibitory effect. From that point of view, the developed mechanism-based PK/PD model may provide a useful tool to gain detailed information on the nature of interaction between buprenorphine and naloxone.

ACKNOWLEDGEMENTS

We gratefully acknowledge the technical assistance of S.M. Bos-van Maastricht. The authors would like to thank Dr. Michael Gautrois and Dr. Rolf Terlinden as well as Ms Nicole Kohl, Mr Klaus Malmendier and Mr Jürgen Weiher for skilful support with the bioanalytical measurements performed in the frame of this work.

REFERENCES

Beal SL and Sheiner LB (1999) NONMEM User's guide. NONMEM Project Group, University of California at San Fransisco, San Fransisco, CA .

Boas RA and Villiger JW (1985) Clinical actions of fentanyl and buprenorphine. The significance of receptor binding. *Br J Anaesth* **57**:192–196.

Bullingham RE, McQuay HJ, Moore A, and Bennett MR (1980) Buprenorphine kinetics. *Clin Pharmacol Ther* **28**:667–672.

Christoph T, Kogel B, Schiene K, Meen M, de Vry J, and Friderichs E (2005) Broad analgesic profile of buprenorphine in rodents of acute and chronic pain. *Eur J Pharmacol* **507**:87–98.

Cleton A, de Greef HJ, Edelbroek PM, Voskuyl RA, and Danhof M (1999) Application of a combined effect compartment/indirect response model to the central nervous system effects of tiagabine in the rat. *J Pharmacokinet Biopharm* **27**:301–323.

Cowan A, Doxey JC, and Harry EJ (1977a) The animal pharmacology of buprenorphine, an oripavine analgesic agent. *Br J Pharmacol* **60**:547–554.

Cowan A, Lewis JW, and Macfarlane IR (1977b) Agonist and antagonist properties of buprenorphine, a new antinociceptive agent. *Br J Pharmacol* **60**:537–545.

Cox D and Oakes D (1984) *Analysis of survival data*. Chapman and Hall, London.

Cox EH, Kerbusch T, Van der Graaf PH, and Danhof M (1998) Pharmacokinetic-pharmacodynamic modeling of the electroencephalogram effect of synthetic opioids in the rat: correlation with the interaction at the mu-opioid receptor. *J Pharmacol Exp Ther* **284**:1095–1103.

D'Amour F and Smith D (1941) A method for determinating loss of pain sensation. *J Pharmacol Exp Ther* **77**:74–79.

Dum JE and Herz A (1981) In vivo receptor binding of the opiate partial agonist, buprenorphine, correlated with its agonistic and antagonistic actions. *Br J Pharmacol* **74**:627–633.

Ette EI, Williams PJ, Kim YH, Lane JR, Liu MJ, and Capparelli EV (2003) Model appropriateness and population pharmacokinetic modeling. *J Clin Pharmacol* **43**:610–623.

Food and Drug Administration (1999) Guidance for industry: Population Pharmacokinetics. Rockville, MD: U.S. Department of Health and Human Services, Food and Drug Administration.

Gal TJ (1989) Naloxone reversal of buprenorphine-induced respiratory depression. *Clin Pharmacol Ther* **45**:66–71.

Henthorn TK, Liu Y, Mahapatro M, and Ng KY (1999) Active transport of fentanyl by the blood-brain barrier. *J Pharmacol Exp Ther* **289**:1084–1089.

Jasinski DR, Pevnick JS, and Griffith JD (1978) Human pharmacology and abuse potential of the analgesic buprenorphine: a potential agent for treating narcotic addiction. *Arch Gen Psychiatry* **35**:501–516.

Jusko WJ, Ko HC, and Ebling WF (1995) Convergence of direct and indirect pharmacodynamic response models. *J Pharmacokinet Biopharm* **23**:5–8; discussion 9–10.

Luks AM, Zwass MS, Brown RC, Lau M, Chari G, and Fisher DM (1998) Opioid-induced analgesia in neonatal dogs: pharmacodynamic differences between morphine and fentanyl. *J Pharmacol Exp Ther* **284**:136–141.

Lutfy K, Eitan S, Bryant CD, Yang YC, Saliminejad N, Walwyn W, Kieffer BL, Takeshima H, Carroll FI, Maidment NT, and Evans CJ (2003) Buprenorphine-induced antinociception is mediated by mu-opioid receptors and compromised by concomitant activation of opioid receptor-like receptors. *J Neurosci* **23**:10331–10337.

Martin WR, Eades CG, Thompson JA, Huppler RE, and Gilbert PE (1976) The effects of morphine- and nalorphine- like drugs in the nondependent and morphine-dependent chronic spinal dog. *J Pharmacol Exp Ther* **197**:517–532.

Mok MS, Lippmann M, and Steen SN (1981) Multidose/observational, comparative clinical analgetic evaluation of buprenorphine. *J Clin Pharmacol* **21**:323–329.

Ohtani M, Kotaki H, Sawada Y, and Iga T (1995) Comparative analysis of buprenorphine- and norbuprenorphine-induced analgesic effects based on pharmacokinetic-pharmacodynamic modeling. *J Pharmacol Exp Ther* **272**:505–510.

Sarton E, Olofsen E, Romberg R, den Hartigh J, Kest B, Nieuwenhuijs D, Burm A, Teppema L, and Dahan A (2000) Sex differences in morphine analgesia: an experimental study in healthy volunteers. *Anesthesiology* **93**:1245–54.

Scott JC, Cooke JE, and Stanski DR (1991) Electroencephalographic quantitation of opioid effect: comparative pharmacodynamics of fentanyl and sufentanil. *Anesthesiology* **74**:34–42.

Sheiner LB, Stanski DR, Vozeh S, Miller RD, and Ham J (1979) Simultaneous modeling of pharmacokinetics and pharmacodynamics: application to d-tubocurarine. *Clin Pharmacol Ther* **25**:358–371.

Shimada S, Nakajima Y, Yamamoto K, Sawada Y, and Iga T (1996) Comparative pharmacodynamics of eight calcium channel blocking agents in Japanese essential hypertensive patients. *Biol Pharm Bull* **19**:430–437.

Stanski DR (1987) Narcotic pharmacokinetics and dynamics: the basis of infusion applications. *Anaesth Intensive Care* **15**:23–26.

Tuk B, Danhof M, and Mandema JW (1997) The impact of arteriovenous concentration differences on pharmacodynamic parameter estimates. *J Pharmacokinet Biopharm* **25**:39–62.

Tuk B, Herben VM, Mandema JW, and Danhof M (1998) Relevance of arteriovenous concentration differences in pharmacokinetic-pharmacodynamic modeling of midazolam. *J Pharmacol Exp Ther* **284**:202–207.

Van der Graaf PH and Danhof M (1997) Analysis of drug-receptor interactions in vivo: a new approach in pharmacokinetic-pharmacodynamic modelling. *Int J Clin Pharmacol Ther* **35**:442–446.

Van der Graaf PH, Van Schaick EA, Visser SA, De Greef HJ, Ijzerman AP, and Danhof M (1999) Mechanism-based pharmacokinetic-pharmacodynamic modeling of antilipolytic effects of adenosine A(1) receptor agonists in rats: prediction of tissue-dependent efficacy in vivo. *J Pharmacol Exp Ther* **290**:702–709.

Verotta D and Sheiner LB (1995) A general conceptual model for non-steady state pharmacokinetic/pharmacodynamic data. *J Pharmacokinet Biopharm* **23**:1–4.

Villiger JW and Taylor KM (1982) Buprenorphine: high-affinity binding to dorsal spinal cord. *J Neurochem* **38**:1771–1773.

Visser SA, Smulders CJ, Reijers BP, Van der Graaf PH, Peletier LA, and Danhof M (2002) Mechanism-based pharmacokinetic-pharmacodynamic modeling of concentration-dependent hysteresis and biphasic electroencephalogram effects of alphaxalone in rats. *J Pharmacol Exp Ther* **302**:1158–1167.

Visser SA, Wolters FL, Gubbens-Stibbe JM, Tukker E, Van Der Graaf PH, Peletier LA, and Danhof M (2003) Mechanism-based pharmacokinetic/pharmacodynamic modeling of the electroencephalogram effects of GABAA receptor modulators: in vitro-in vivo correlations. *J Pharmacol Exp Ther* **304**:88–101.

Walsh SL, Preston KL, Stitzer ML, Cone EJ, and Bigelow GE (1994) Clinical pharmacology of buprenorphine: ceiling effects at high doses. *Clin Pharmacol Ther* **55**:569–580.

Watson PJ, McQuay HJ, Bullingham RE, Allen MC, and Moore RA (1982) Single-dose comparison of buprenorphine 0.3 and 0.6 mg i.v. given after operation: clinical effects and plasma concentration. *Br J Anaesth* **54**:37–43.

Zhang AZ and Pasternak GW (1981) Opiates and enkephalins: a common binding site mediates their analgesic actions in rats. *Life Sci* **29**:843–851.

Zuideveld KP, Van der Graaf PH, Newgreen D, Thurlow R, Petty N, Jordan P, Peletier LA, and Danhof M (2004) Mechanism-based pharmacokinetic-pharmacodynamic modeling of 5-HT1A receptor agonists: estimation of in vivo affinity and intrinsic efficacy on body temperature in rats. *J Pharmacol Exp Ther* **308**:1012–1020.

Zuideveld KP, Rusic-Pavletic J, Maas HJ, Peletier LA, Van der Graaf PH, and Danhof M (2002) Pharmacokinetic-pharmacodynamic modeling of buspirone and its metabolite 1-(2-pyrimidinyl)-piperazine in rats. *J Pharmacol Exp Ther* **303**:1130–1137.

FOOTNOTES

Financial support by Grünenthal GmbH, Aachen, Germany is gratefully acknowledged.

Figure 1. A schematic view of the mechanism-based PK/PD model. The model incorporates different processes to explain time dependencies in pharmacodynamics. The pharmacokinetics describe the disposition of the drug in the plasma and equilibration to the biophase site. At the target site, the drug can bind to the receptor. Upon binding to the receptor, a cascade of transduction processes are activated, ultimately leading to a pharmacological response.

Figure 2. Individual buprenorphine concentration-time profiles for the treatment groups I-V. The observed concentrations (closed circles) and population predictions (thick line) are depicted. The black boxes represent the duration of infusion.

Figure 3. Individual fentanyl concentration-time profiles for the treatment groups I-V. The observed concentrations (closed circles) and population predictions (thick line) are depicted. The black boxes represent the duration of infusion.

Figure 4. Results of the posterior predictive performance of the population PK models of buprenorphine (left panel) and fentanyl (right panel) for the different treatment groups. The observed concentration (closed circles,) 2.5 % quantile (lower solid line), median value (dashed line) and 97.5 % quantile (upper solid line) are presented. The black boxes represent the duration of infusion. The influence of bodyweight on the pharmacokinetics of buprenorphine and fentanyl was also taken into account. Bodyweight was simulated for each animal assuming inter-animal variability of bodyweight is 3.5 % (normal distribution) and mean bodyweight is 0.300 kg.

Figure 5. Changes in tail flick latency in time following administration of buprenorphine. For each treatment group (I-V) the observed (closed circles) and predicted (solid line) time course of antinociceptive effect is shown.

Figure 6. Changes in tail flick latency in time following administration of fentanyl. For each treatment group (I-V) the observed (closed circles) and predicted (solid line) time course of

antinociceptive effect is shown.

Figure 7. Panel A: *Concentration-receptor binding relationship*.The relationship between effect-site concentration and receptor binding for buprenorphine for all rats. Effect-site concentration (ng/ml) is depicted on the x-axis on a logarithmic scale and receptor binding, expressed as fractional receptor occupancy, is depicted at the y-axis. The closed circles represent the predicted receptor binding. Panel B: *receptor binding-effect relationship*. The receptor binding *vs.* effect relationship as described by equation 9 for buprenorphine for all rats. The closed circles represent the predicted tail flick latency. Panel C: *fentanyl concentration-effect relationship*. The fentanyl effect-site concentration *vs.* tail flick latency relationship as described by equation 10. The closed circles represent the predicted tail flick latency. The solid line displays the cut-off tail flick latency time.

Figure 8. Representative individual concentration *vs.* time profiles for buprenorphine and its metabolite norbuprenorphine. The observed buprenorphine concentrations (closed circles), norbuprenorphine concentrations (closed triangles) and individual predicted buprenorphine concentrations (dashed line) are depicted.

JPET Fast Forward. Published on February 8, 2005 as DOI: 10.1124/jpet.104.082560
This article has not been copyedited and formatted. The final version may differ from this version.

Table 1. Experimental design of the study describing the PK-PD relationship of the antinociceptive effect of buprenorphine and fentanyl, with respect to number of animals per treatment group and their corresponding dose normalized for body weight, absolute dose, length of infusion and body weight. Data are presented as mean ± S.E.

Group	n	Infusion time (min)	Dose (mg/kg)	Absolute Dose (mg)	body weight (kg)
			buprenorphine		
I	5	20	0.015	0.0043 ± 0.0002	0.288 ± 0.011
II	8	20	0.030	0.0081 ± 0.0003	0.271 ± 0.010
III	7	40	0.030	0.0088 ± 0.0006	0.293 ± 0.020
IV	8	20	0.060	0.0160 ± 0.0018	0.267 ± 0.029
V	7	20	0.10	0.0276 ± 0.0027	0.276 ± 0.027
Control[1]	4	20	-	-	0.283 ± 0.011
Control	4	40	-	-	0.289 ± 0.015
			fentanyl		
I	8	20	0.020	0.0052 ± 0.0002	0.262 ± 0.010
II	8	20	0.025	0.0067 ± 0.0004	0.268 ± 0.015
III	8	20	0.035	0.0089 ± 0.0005	0.254 ± 0.015
IV	8	40	0.035	0.0095 ± 0.0007	0.270 ± 0.019
V	8	20	0.040	0.0106 ± 0.0008	0.265 ± 0.021
Control[2]	4	20	-	-	0.278 ± 0.025
Control	4	40	-	-	0.263 ± 0.018

[1] Control groups received an infusion of saline containing polysorbate 80.

[2] Control groups received an infusion of saline.

JPET Fast Forward. Published on February 8, 2005 as DOI: 10.1124/jpet.104.082560
This article has not been copyedited and formatted. The final version may differ from this version.

Table 2. Parameter estimates of the final population pharmacokinetic model for buprenorphine and the stability of the parameters using the bootstrap resampling procedure

	Original data set		1000 bootstrap replicates	
	Estimate	% CV	Estimate	% CV
Structural model				
Cl, *ml/min/kg*				
$\Theta_{intercept}$	14	2.4	14	2.6
Θ_{slope}	95	32	95	30
V_1, *ml/kg*				
$\Theta_{intercept}$	120	7.6	113	7.4
Θ_{slope}	2150	3.9	2080	3.9
V_2, *ml/kg*				
$\Theta_{intercept}$	300	20	306	16
Θ_{slope}	2900	5.3	2920	5.0
V_3, *ml/kg*				
$\Theta_{intercept}$	810	13	812	14
Θ_{slope}	3900	31	3960	34
Q_2, *ml/min*	26.0	18	27.0	20
Q_3, *ml/min*	7.3	30	7.28	31
Inter-animal variability				
ω*Cl*, %	12	36	12	39
ωV_1, %	60	61	68	76
ωV_2, %	19	41	18	44
ωV_3, %	10	46	10	53
Residual variability				
proportional error, %	13	10	13	11

JPET Fast Forward. Published on February 8, 2005 as DOI: 10.1124/jpet.104.082560
This article has not been copyedited and formatted. The final version may differ from this version.

Table 3. Parameter estimates of the final population pharmacokinetic model for fentanyl and the stability of the parameters using the bootstrap resampling procedure

	Original data set		1000 bootstrap replicates	
	Estimate	% CV	Estimate	% CV
Structural model				
Cl, ml/min/kg				
$\Theta_{intercept}$	16.4	2.5	16.4	2.9
Θ_{slope}	135	19	127	22
V_1, *ml*	197	8.3	196	8.9
V_2, *ml*	443	4.8	443	4.6
Q, ml/min	14.5	5.7	14.5	5.9
Inter-animal variability				
ω*Cl*, %	13	22	13	23
ωV_1, %	43	30	42	35
ωV_2, %	20	28	19	28
Corr ω^2_{Cl} , ω^2_{V2}	0.70			
Residual variability				
proportional error, %	20	9.0	20	8.9

JPET Fast Forward. Published on February 8, 2005 as DOI: 10.1124/jpet.104.082560
This article has not been copyedited and formatted. The final version may differ from this version.

Table 4. Linear regression equations describing the relationship between pharmacokinetic parameters and bodyweight (kg)

Fentanyl		
Cl, ml/min/kg	=	$16.4 + 135 \cdot (BW - 0.263)$
Buprenorphine		
Cl, ml/min/kg	=	$14 + 95.0 \cdot (BW - 0.281)$
V_1, *ml/kg*	=	$120 + 2150 \cdot (BW - 0.281)$
V_2, *ml/kg*	=	$300 + 2900 \cdot (BW - 0.281)$
V_3, *ml/kg*	=	$810 + 3900 \cdot (BW - 0.281)$

JPET Fast Forward. Published on February 8, 2005 as DOI: 10.1124/jpet.104.082560
This article has not been copyedited and formatted. The final version may differ from this version.

Table 5. Population pharmacodynamic estimates and inter-animal variability of buprenorphine. For the fixed and random parameter estimates the coefficient of variation (CV) is displayed.

Parameter	Population estimate	CV of parameter estimate (%)	Inter-animal variability (CV %)	CV of variability estimate (%)
k_{on}, *ml/ng/min*	0.0228	21.9	-[1]	-
k_{off}, min^{-1}	0.0731	21.5	49	23
K_D[2], *ng/ml*	3.20	-	-	-
k_{eo}, min^{-1}	0.0242	12.2	45	29
E_0, *s*	3.09	1.4	7	36
Z	14	7.9	-	-

[1] - = not estimated

[2] secondary parameter ($K_D = k_{off}/k_{on}$)

JPET Fast Forward. Published on February 8, 2005 as DOI: 10.1124/jpet.104.082560
This article has not been copyedited and formatted. The final version may differ from this version.

Table 6. Population pharmacodynamic estimates and inter-animal variability of fentanyl. For the fixed and random parameter estimates the coefficient of variation (CV) is displayed.

Parameter	Population estimate	CV of parameter estimate (%)	Inter-animal variability (%)	CV of variability estimate (%)
k_{eo}, min^{-1}	0.123	11.6	63	37
$C_{100}, ng/ml$	3.51	7.3	39	19
E_0, s	2.79	1.9	9	35
γ	1.16	5.3	26	49
Z	17.5	5.9	- [1]	-

[1] - = not estimated

JPET Fast Forward. Published on February 8, 2005 as DOI: 10.1124/jpet.104.082560
This article has not been copyedited and formatted. The final version may differ from this version.

Table 7. The goodness-of-fit, judged by objective function value, of three population PK/PD models containing expressions for the kinetics of onset and offset of buprenorphine and fentanyl. The population PK/PD models incorporate biological processes causing time-dependencies (biophase equilibration, receptor binding kinetics) in the pharmacodynamics of buprenorphine and fentanyl. For buprenorphine hysteresis is explained on the basis of kinetics of target site distribution and receptor association/dissociation kinetics.

	objective function value	
	buprenorphine	fentanyl
biophase equilibration model	-283.1	-378.2
receptor binding model	-241.2	-322.4
biophase equilibration/receptor binding model	-523.9	-378.0

JPET Fast Forward. Published on February 8, 2005 as DOI: 10.1124/jpet.104.082560
This article has not been copyedited and formatted. The final version may differ from this version.

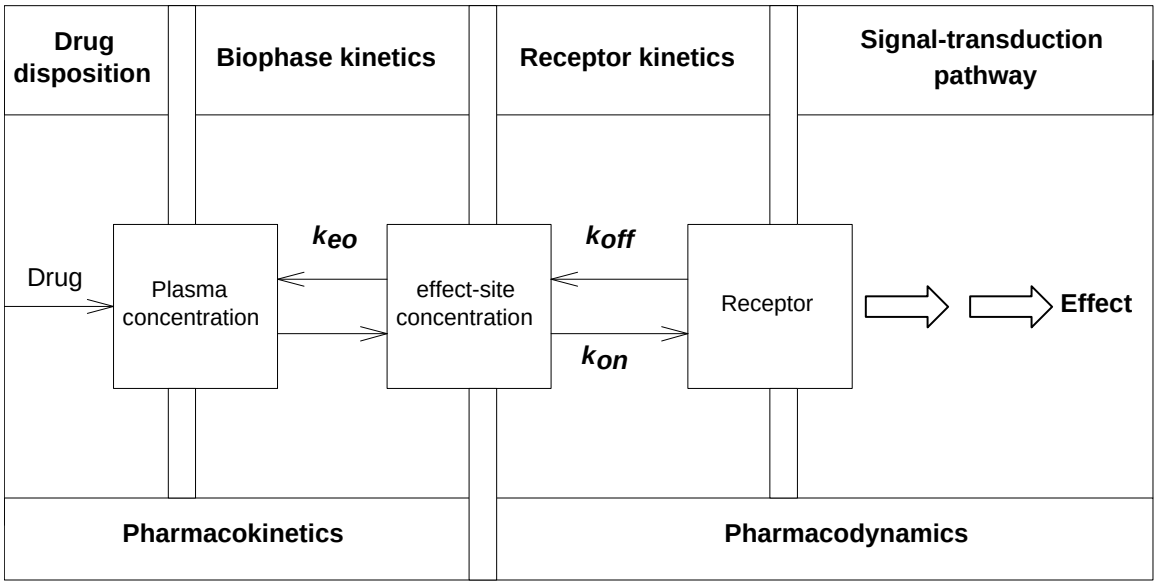

Figure 1

JPET Fast Forward. Published on February 8, 2005 as DOI: 10.1124/jpet.104.082560
This article has not been copyedited and formatted. The final version may differ from this version.

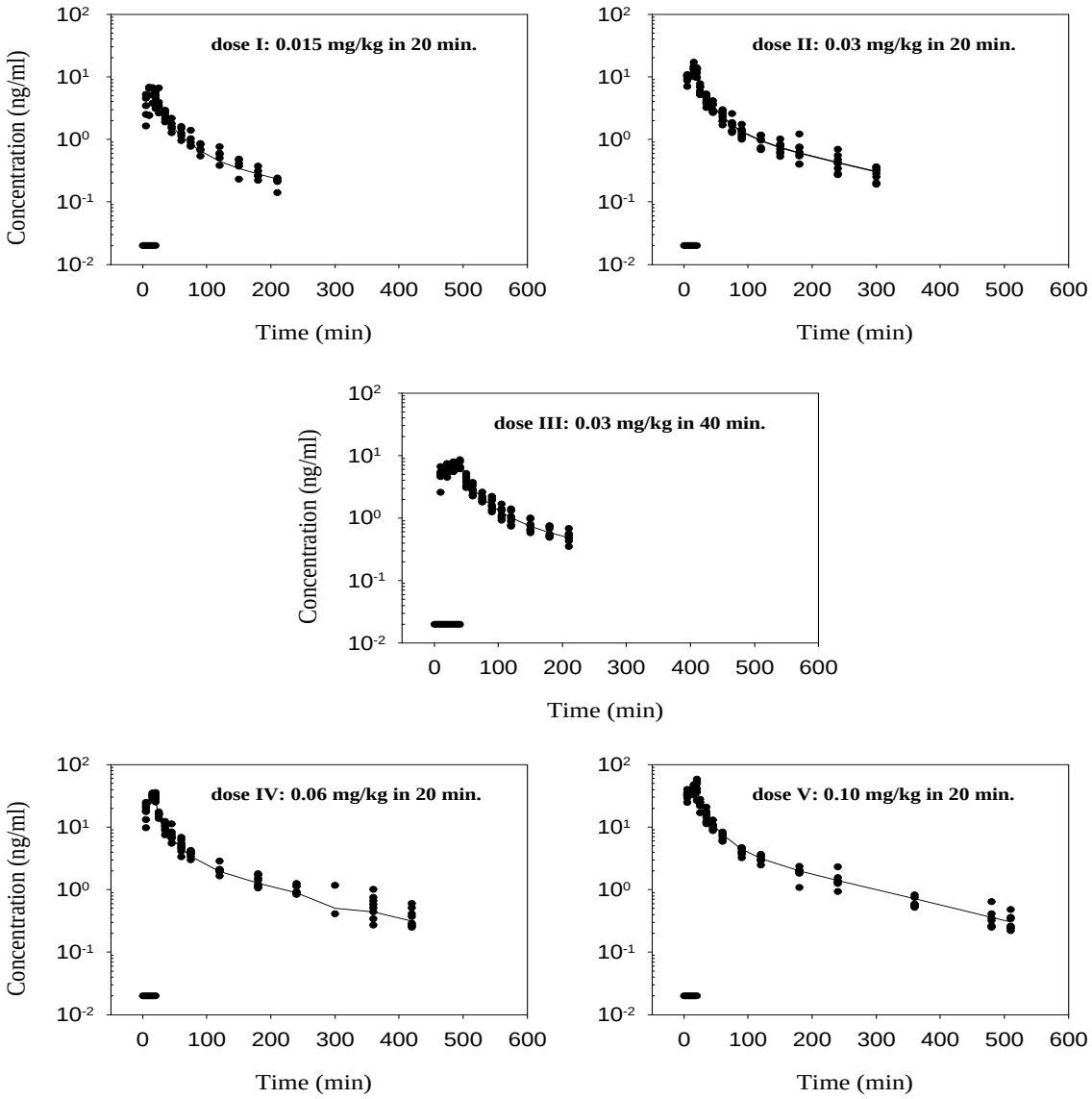

Figure 2

JPET Fast Forward. Published on February 8, 2005 as DOI: 10.1124/jpet.104.082560
This article has not been copyedited and formatted. The final version may differ from this version.

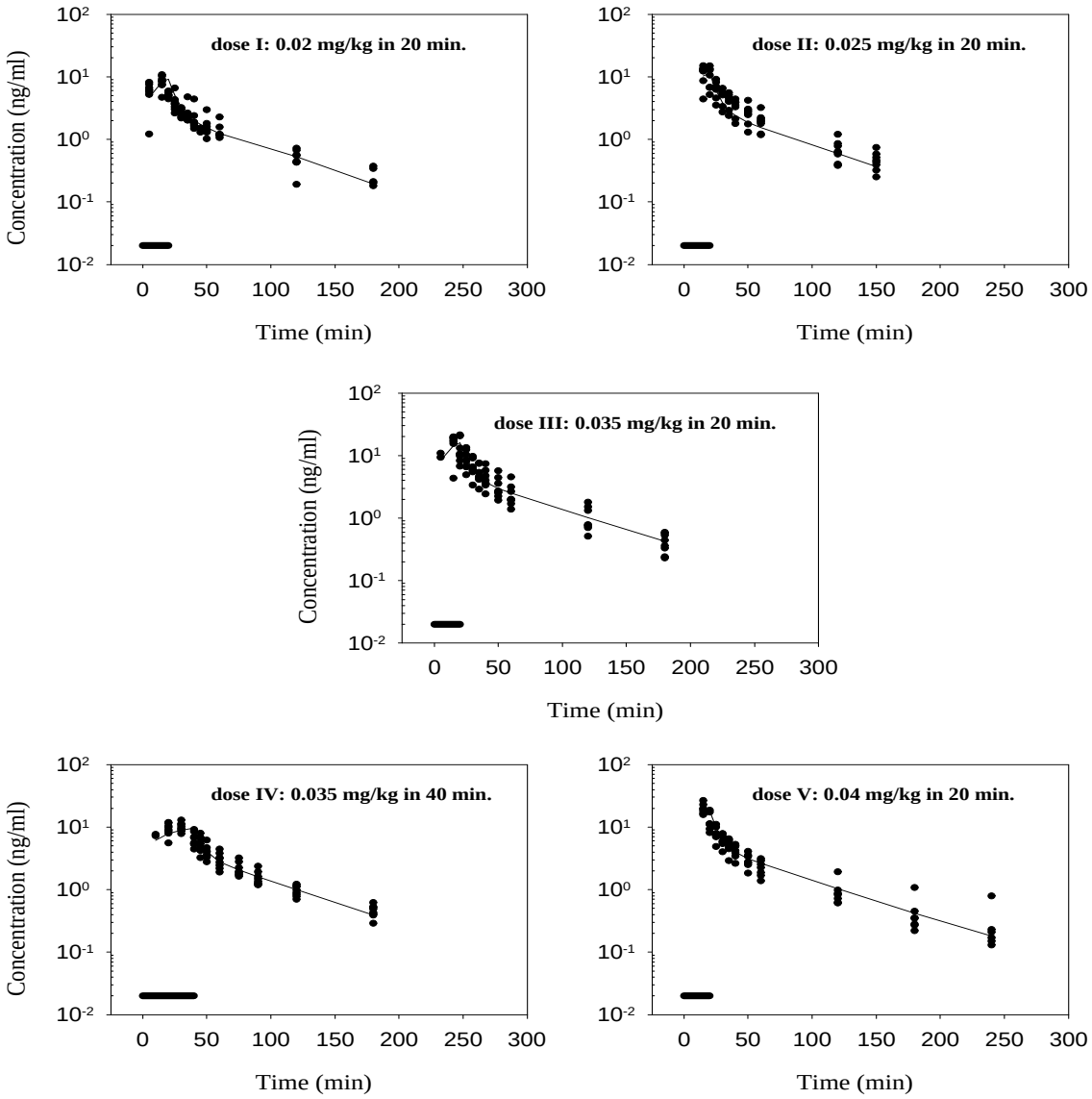

Figure 3

JPET Fast Forward. Published on February 8, 2005 as DOI: 10.1124/jpet.104.082560
This article has not been copyedited and formatted. The final version may differ from this version.

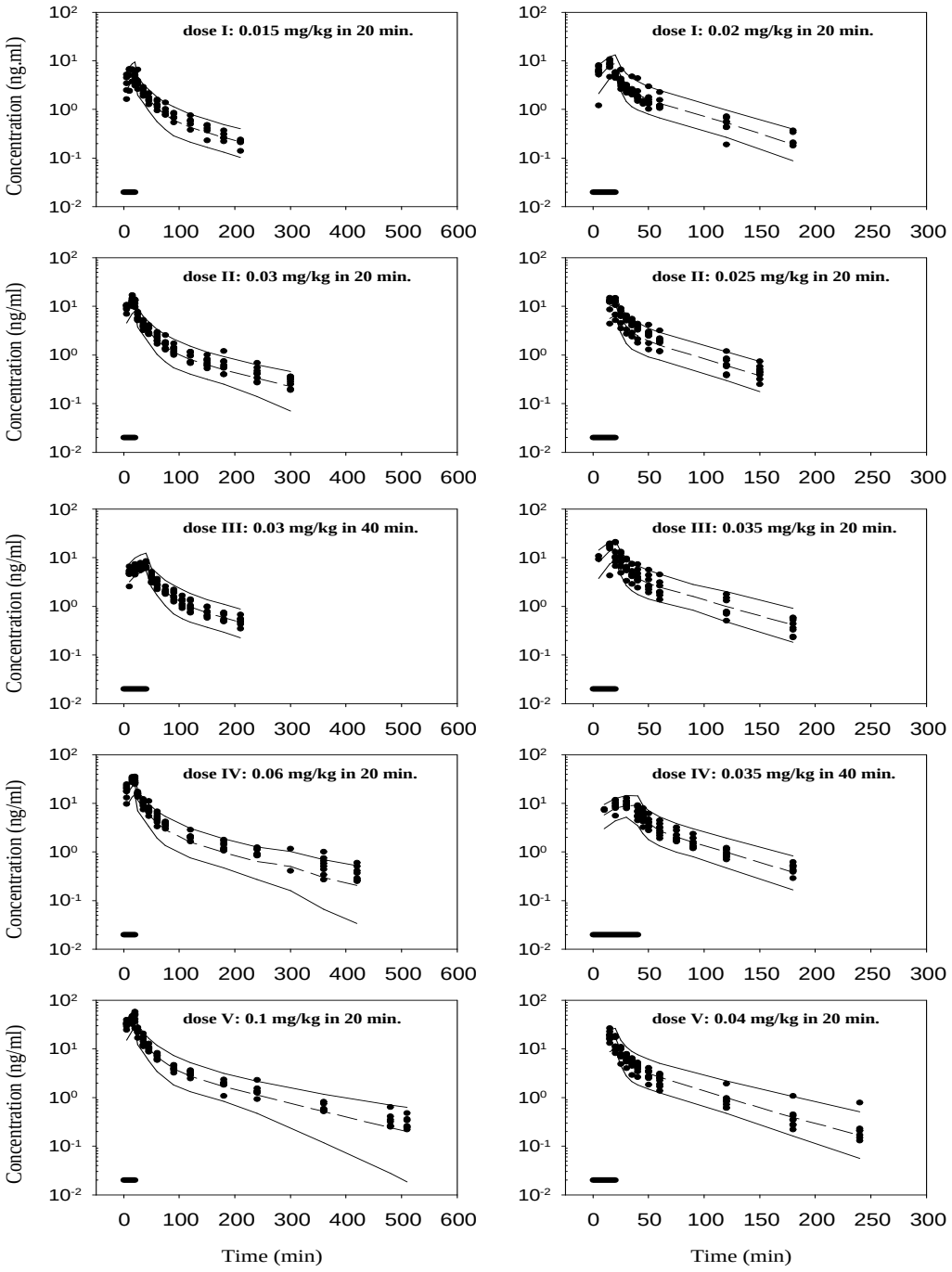

Figure 4

JPET Fast Forward. Published on February 8, 2005 as DOI: 10.1124/jpet.104.082560
This article has not been copyedited and formatted. The final version may differ from this version.

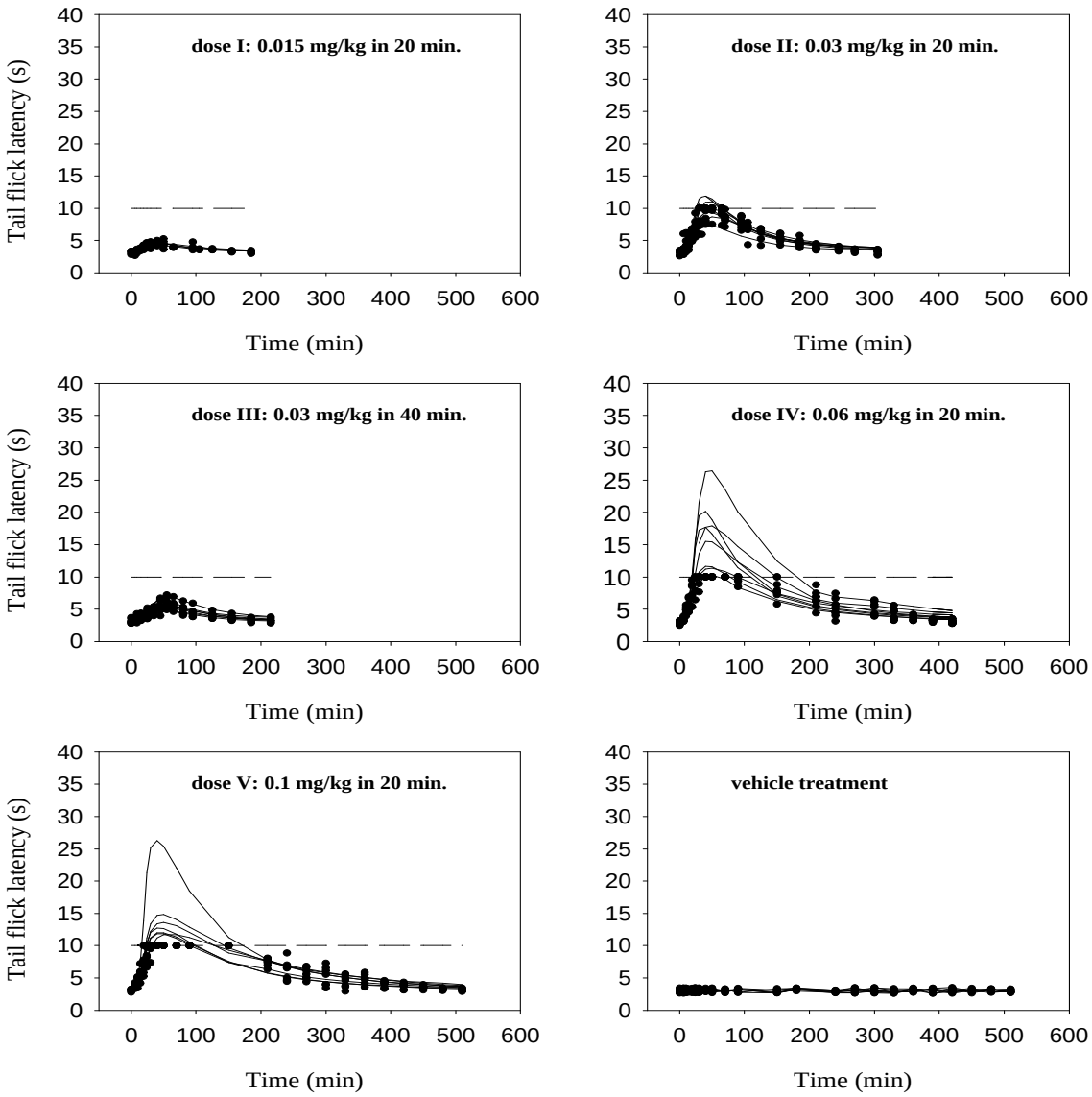

Figure 5

JPET Fast Forward. Published on February 8, 2005 as DOI: 10.1124/jpet.104.082560
This article has not been copyedited and formatted. The final version may differ from this version.

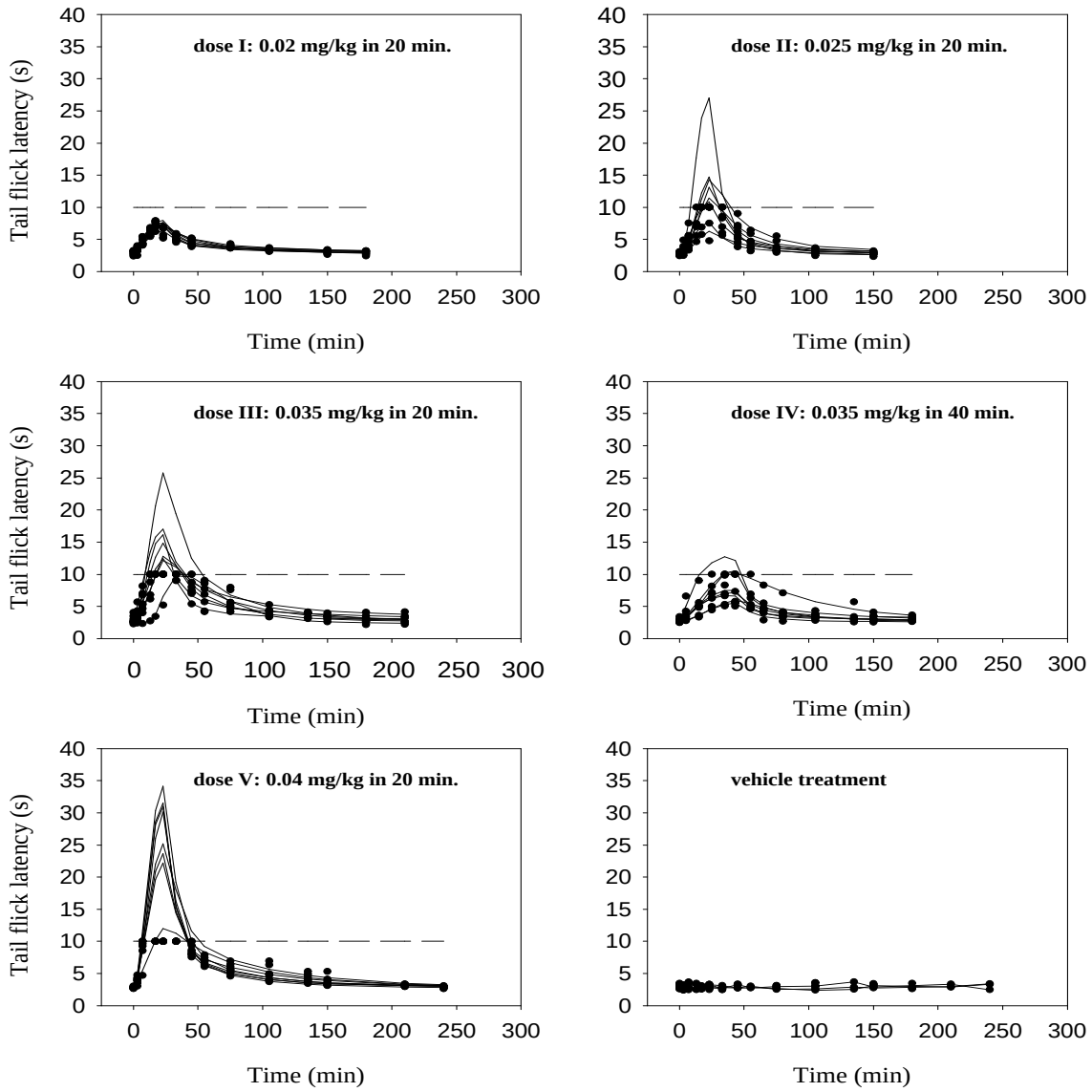

Figure 6

JPET Fast Forward. Published on February 8, 2005 as DOI: 10.1124/jpet.104.082560
This article has not been copyedited and formatted. The final version may differ from this version.

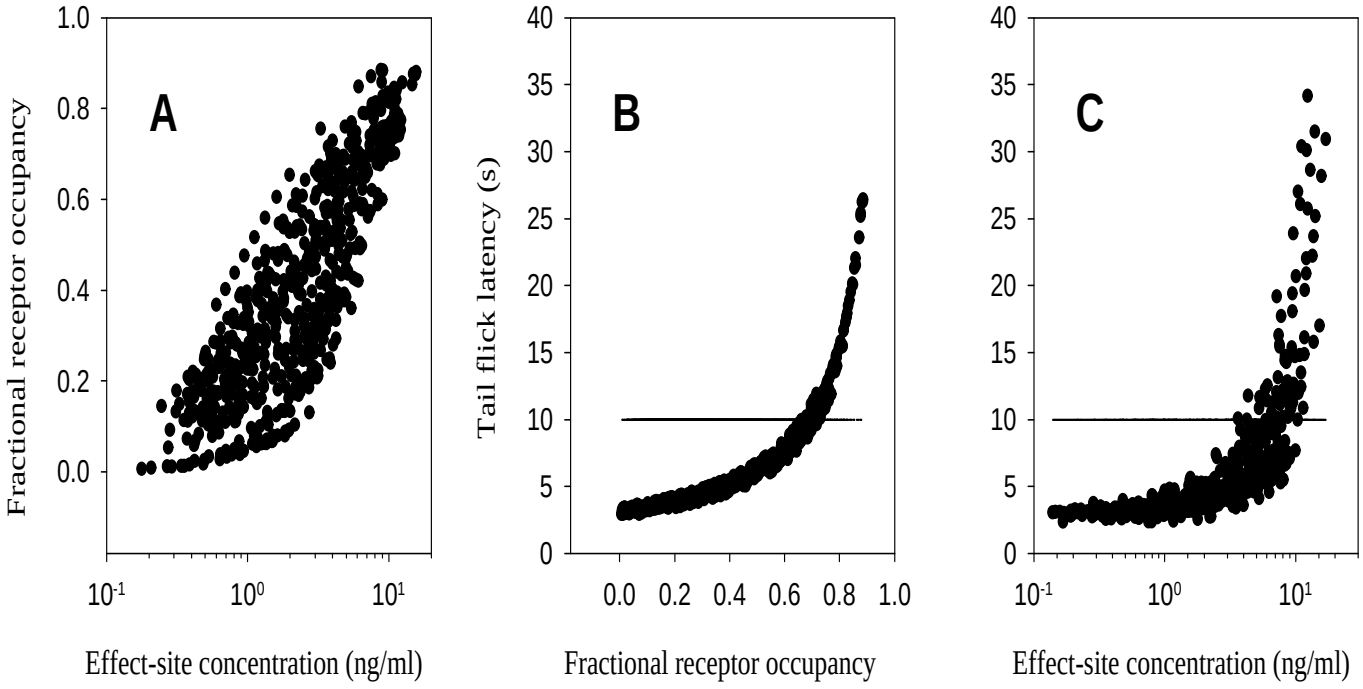

Figure 7

JPET Fast Forward. Published on February 8, 2005 as DOI: 10.1124/jpet.104.082560
This article has not been copyedited and formatted. The final version may differ from this version.

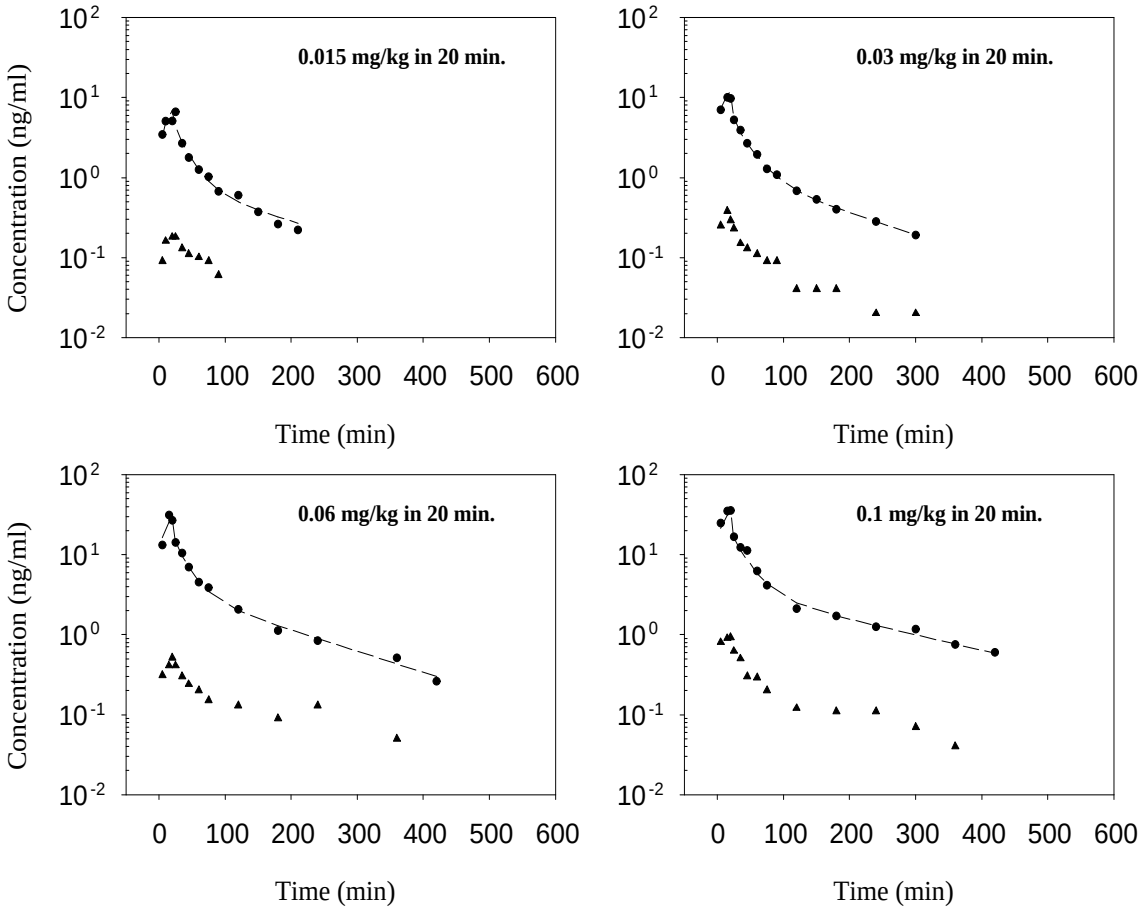

Figure 8